

CONTINUOUS OPERATION OF CRYOGENIC CURRENT COMPARATORS AT FAIR*

T. Sieber[†], M. Schwickert, GSI, Darmstadt, Germany

S. Shinde¹, F. Schmidl, Friedrich-Schiller-University Jena, Jena, Germany

T. Stoehlker^{1,2}, V. Tympel¹, Helmholtz Institute Jena, Jena, Germany

T. Koettig, CERN European Organization for Nuclear Research, Geneva, Switzerland

¹also at GSI Helmholtz Centre for Heavy Ion Research, Darmstadt, Germany

²also at Institute for Optics and Quantum Electronics, Jena, Germany

Abstract

Cryogenic Current Comparators (CCC) are superconducting devices for beam current monitoring, based on azimuthal magnetic field (fT range) measurement with ultra-sensitive SQUID magnetometers. They are able to provide a calibrated non-destructive measurement of beam current with a resolution of 10 nA or better, independent from ion species and without tedious calibrations procedure.

We have developed the CCC over the last ten years in an international collaboration with the goal of a highly sensitive and continuous current measurement in the transfer lines and rings at FAIR and CERN machines. Besides the efforts to improve the robustness and current resolution of the device, investigations have been performed on the cryogenic support system, which has to provide stand-alone operation in HEBT tunnels without He supply. So far, we have achieved standing times in the range of 6 - 9 months after liquid He filling, recently we have demonstrated stand-alone He liquefaction from gas bottles within ~ 4 weeks, which would avoid He filling in the tunnels. In this contribution we present the status and results of our current work with focus on the cryogenics aspects.

INTRODUCTION

The Cryogenic Current Comparator basically consists of a pickup coil, a SQUID- (Superconducting Quantum Interference Device) magnetometer and a superconducting shielding, which provides an attenuation of non-azimuthal external fields in the range -70 dB to -140 dB, depending on the shield geometry (see below). The shielding guides the superconducting Meissner-Current to the internal pickup loop, which is basically a one-winding coil around a high permeability ring core, acting as a flux concentrator. The latter is used in the 'classical' CCC, shown in Fig. 1, to ensure efficient coupling of the beam to the SQUID circuit. Just like in regular, normal conducting beam transformers, the arrangement can be regarded as a transformer with the particle beam being the primary and the pickup coil being the secondary winding. The signal from the pickup coil is fed to a DC SQUID, which is operated in a compensation circuit, using a so-called Flux Locked Loop

(FLL) electronics [1]. Figure 1 shows the original arrangement, developed at PTB (Physikalisch-Technische Bundesanstalt) for electron beam measurement [2], which was later adapted to the heavy ion accelerator application at GSI [3].

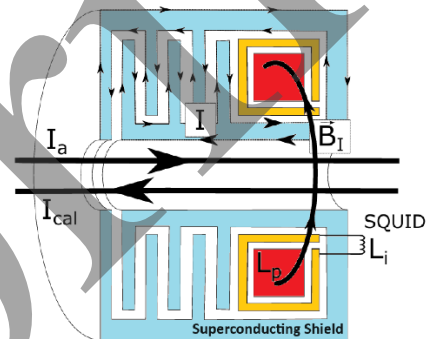


Figure 1: Classical current comparator, shield geometry with radial meanders and high permeability ring core (red) surrounded by the pickup loop (yellow), which is again connected to the SQUID coupling loop. In our case the reference current is not used, I_a is the beam current. B_i = azimuthal field, L_i = coupling inductance to squid circuit. The small arrows indicate the Meissner current along the shielding.

The detector development for FAIR started with the classical shielding, like shown in Fig.1. The next step was a shielding with axial meander geometry and without ring core [4], called the 'coreless' or 'axial' CCC. This new design promised some advantages, like reduced magnetic noise and baseline drift (both mainly caused by the toroidal core), reduced costs and weight due to better mechanical stability (which allows for lead as shielding material). However, the axial CCC could not be operated inside the FAIR cryostat due to its sensitivity to external noise and in general its weak coupling to beam (resp. calibration-) current [5]. Consequently, a third CCC type, which combines the axial meander geometry with a twofold classical toroidal core pickup was developed [6] and successfully tested with beam at GSI [7]. It achieved - besides excellent magnetic shielding - a current resolution equal or better than the classical CCC type. This version is called the 'dual

* supported by BMBF under contracts 05P18SJR1 and 05K25SJA

[†]T.Sieber@gsi.de

core' or DCCC. Figure 2 shows the three mentioned varieties at one glance.

The DCCC represents a preliminary conclusion of our detector development and is the final choice for the FAIR diagnostics system. Some further optimization is ongoing to improve synchronization of the SQUIDS as well as for filtering of periodic disturbances [8], but the basic detector design is fixed. The dimensions of the DCCC for FAIR are: inner diameter $D_{inner} = 255$ mm, $D_{outer} = 360$ mm, length $l = 230$ mm. It reaches a current resolution of several nA at a bandwidth of 10 kHz.

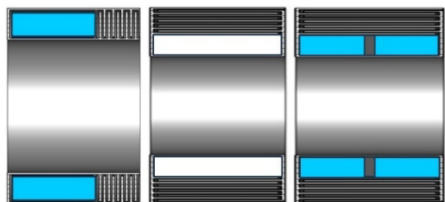


Figure 2: CCC shielding types with radial (left) and axial (middle) meanders. The high permeability ring-cores are indicated in blue, the detector volume of the axial CCC in white. Right: DCCC with axial meanders and two independent toroidal cores.

CRYOGENIC SUPPORT SYSTEM

A major requirement for stable nonstop operation in the FAIR beamlines (and the remaining challenge) is complete self-contained stand-alone operation of the cryogenic system. To achieve this, the cryogenic support system has steadily been optimized in parallel to the work on the detectors [9].

The basis of the cryo-system is the specially developed He bath cryostat shown in Fig. 3.

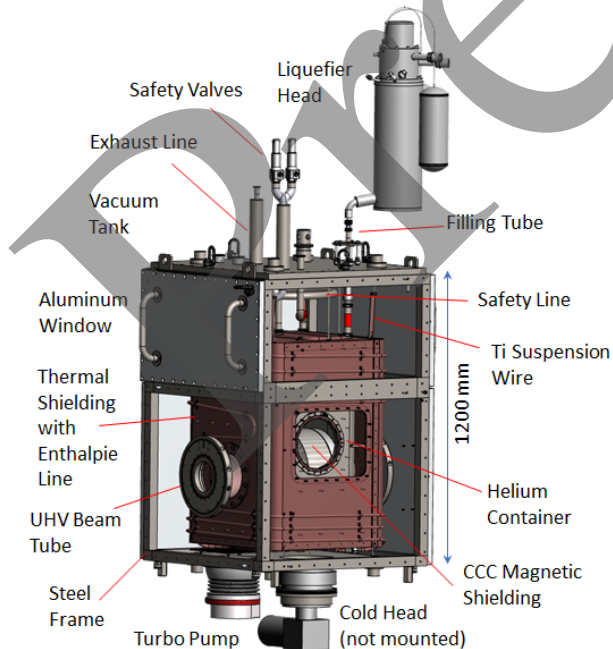


Figure 3: FAIR CCC cryostat with Cryomech© HeRL25 liquefier mounted.

Immersion in LHe fulfils the requirements of maximum stability and homogeneous cooling. In addition, the cryostat has to provide UHV suitability, nonmagnetic material, vibrational damping, short insertion length as well as accessibility for maintenance and repair work. The outer dimensions of the isolation vacuum vessel are 1.2 m x 0.8 m x 0.8 m. It consists of a stainless-steel frame, covered by aluminum windows, which enable access to all inner components. The He container (volume 70 l), which houses the CCC is located in the center and is fixed by (Ti) suspension wires, anchored in the corners of the isolation vacuum tank. It is surrounded by a thermal shielding made from copper, which is cooled by the evaporated helium (enthalpy cooling). The enthalpy line spiraling around the thermal shield has a length of ~ 15 m at an inner diameter of 10 mm. Shield temperature during operation is ~ 110 K at an evaporation rate of ~ 20 l/day.

The circulation of the gas is powered by the thermosiphon effect from density reduction/liquefaction at the liquefier cold head. Once it is running, there are two competing ways for the gas flow, 1. along the shield cooling line (as intended), 2. backwards through the He filling tube.

Calculations predict an evaporation rate of 17 l/day. Table 1 shows the main heat contributions.

Table 1: Heat Contribution from Cryostat Components

Cryostat Component	Heat Load [W]
Suspensions 8 x TiAl6V4, 3mm	0.03
He Filling Tube, Stainless Steel/GFK	0.25
Tube for Sensor and CCC Cables	0.01
Overpressure Safety Tube	0.03
He Filling Rod	~ 0.08
Sensor and CCC Cables	~ 0.07
Radiation on He Vessel ($T_{shield} = 100$ K)	0.05
Radiation on He Tube ($T_{shield} = 100$ K)	0.01
Total Heat Load	~ 0.53
\Rightarrow Evaporation Rate	~ 17 l/day

CLOSED CYCLE OPERATION

A system for gas handling and re-liquefaction has been installed to achieve self-contained operation. Fig. 4 shows a schematic of our test setup. We started our tests with a Cryomech© HeRL15 He-liquefier (capacity 15l/day). It turned out the additional heat load by the liquefier filling tube itself made it necessary to switch to a more powerful model (HeRL25). After several optimization steps (e.g. installation of metal seals at all ISO-KF flanges, a check valve at recovery line and installation of flow meters for gas flow optimization) we managed to get the system running in (almost) stand-alone mode. We started the test campaign in Nov24 and finally ran out of helium mid May25. The filling level at start was around 50 l.



Figure 4: Cryogenic system of the CCC. Flow meters detect the flow to recovery line and liquefier. An additional He supply bottle compensates losses. Operation pressure is at 1.1 bara.

Further investigations are necessary to identify loss (or contamination) mechanisms in the He circuit. Avoiding contaminations and losses can be achieved by careful choice of material and systematic work, which is comparatively simple though not trivial. In contrast, investigation of the dynamical behavior is complicated. The cryostat is a complex system, with a large number of coupled parameters, which are again time and temperature dependent. A simple estimate of the heat load, like in table 1, shows only small part of the boundary conditions. In reality the system will after He filling start to oscillate over different modes, reaching at some point an equilibrium, which still includes two or more superimposed oscillations. Figure 5 shows as an example the oscillations over a period of 1 ½ hours during our liquefaction test.

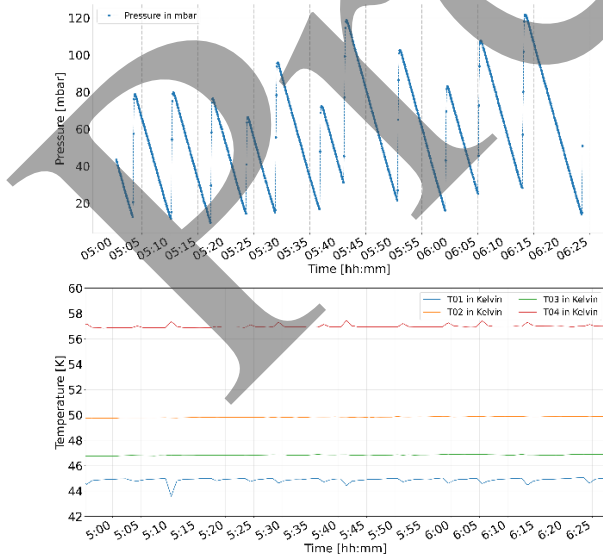


Figure 5: Pressure oscillations during a liquefaction test (upper). The temperatures of He chamber and shield are oscillating accordingly (lower).

We assume that the oscillations are mainly driven by the contest of gas flow through the thermal shield and through the liquefier filling rod. The LHe is released periodically from the liquefier, once it evaporates in the He container, the cold gas will gradually reduce the resistivity of the enthalpy line (while partly streaming back through the filling rod), which increases the amount of warm gas coming to the liquefier. Here - due to limited power at 4K - a certain time span is needed to start the cycle again. Temperature values from shield and cold head are in agreement with this interpretation.

For better understanding of the thermal properties and gas dynamics, we are developing a thermodynamic model. The simulation workflow starts from the CCC CAD assembly provided as a STEP model and generates meshes at two levels. A surface mesh is produced for interactive 3D visualization and is rendered in a WebGL GLB viewer, enabling inspection of the cryogenic subassemblies and their thermal state. In parallel, a volumetric mesh is generated to serve as the computational domain for the physics solver.

Due to the geometric complexity and limited computing resources, the surface and volumetric meshing are treated as separate steps. The governing thermodynamic and control equations are then advanced in time using open-source Python libraries, and the resulting state variables (e.g., temperatures, boil-off/liquefaction rate, and pressure dynamics) are used both for quantitative analysis and for mapping temperature fields back onto the visualization mesh for interpretation of system behaviour. Figure 6 shows a calculated gas flow for different components [10].

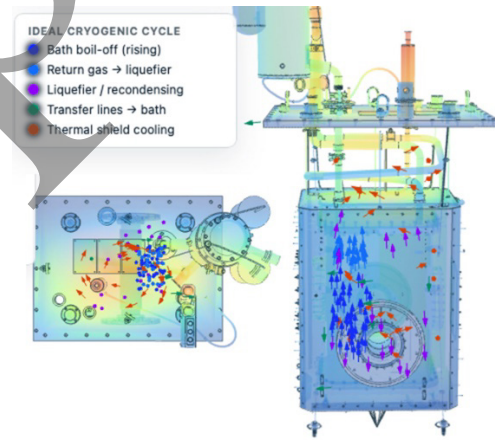


Figure 6: Simulation of gas flow in the cryostat / liquefier system. Left: top view, right: side view.

SUMMARY AND OUTLOOK

CCC development on detector side is preliminary concluded with the dual core DCCC as final design choice. The remaining task to allow for routine operation of the CCC in FAIR tunnels is to stabilize the cryogenic support system and to demonstrate stand-alone operation. We achieved six months standing time, showing that the liquefier power is sufficiently high. We are developing a numerical model of the cryostat to investigate the He consumption and the dynamic behavior of the system.

REFERENCES

- [1] F. Kurian, “Cryogenic Current Comparators for precise Ion Beam Current Measurements”, PhD thesis, University of Frankfurt, Germany, 2015K.
- [2] Grohmann, H. D. Hahlbohm, D. Hechtfischer, and H. Lübbig, “Field attenuation as the underlying principle of cryocurrent comparators 2. Ring cavity elements”, *Cryogenics*, vol. 16, no. 10, pp. 601–605, 1976.
[doi:10.1016/0011-2275\(76\)90192-2](https://doi.org/10.1016/0011-2275(76)90192-2)
- [3] A. Peters *et al.*, “A Cryogenic Current Comparator for the absolute Measurement of nA Beams”, *AIP Conf. Proc.*, vol. 451 pp.163-180, 1998. [doi:10.1063/1.56997](https://doi.org/10.1063/1.56997)
- [4] V. Zakosarenko *et al.*, “Coreless SQUID-based cryogenic current comparator for non-destructive intensity diagnostics of charged particle beams”, *Supercond. Sci. Technol.*, vol. 32, pp. 014002, Dec. 2018.
[doi: 10.1088/1361-6668/aaf206](https://doi.org/10.1088/1361-6668/aaf206)
- [5] D. M. Haider *et al.*, “Versatile Beamline Cryostat for the Cryogenic Current Comparator (CCC) for FAIR”, in *Proc. IBIC'19*, Malmö, Sweden, pp. 78-81, Sep. 2019.
[doi:10.18429/JACoW-IBIC2019-MOPP007](https://doi.org/10.18429/JACoW-IBIC2019-MOPP007)
- [6] Max Stapelfeld, „Experimentelle Untersuchungen zum Systemdesign von Kryogenen Stromkomparatoren“, PhD thesis Friedrich Schiller University Jena, Germany, 2022
- [7] L. Crescimbeni, “Development of the axial Cryogenic Current Comparator for FAIR”, PhD thesis, University of Frankfurt, Germany, 2025 (in preparation)
- [8] S. Kolbe, F. Römer, T. Sieber, V. Tympel, and B. Voss, “Systematic analysis and mitigation of disturbances in beam current measurements using dual SQUID readout”, presented at the IPAC'26, Deauville, France, May 2026, paper WEP6044, this conference.
- [9] T. Sieber *et al.*, “Optimization Studies for an Advanced Cryogenic Current Com parator (CCC) System for FAIR”, in *Proc. IBIC'16*, Barcelona, Spain, Sep. 2016, pp. 715-718.
[doi:10.18429/JACoW-IBIC2016-WEPG40](https://doi.org/10.18429/JACoW-IBIC2016-WEPG40)
- [10] S. Shinde *et al.*, “Thermodynamic Simulations for the Cryogenic Current Comparator”, to be presented at IBIC'26, Whistler, Canada, Sep. 2026